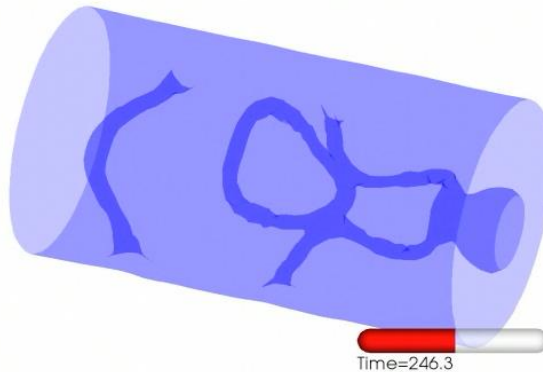
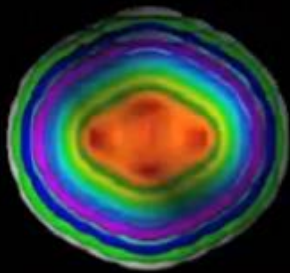
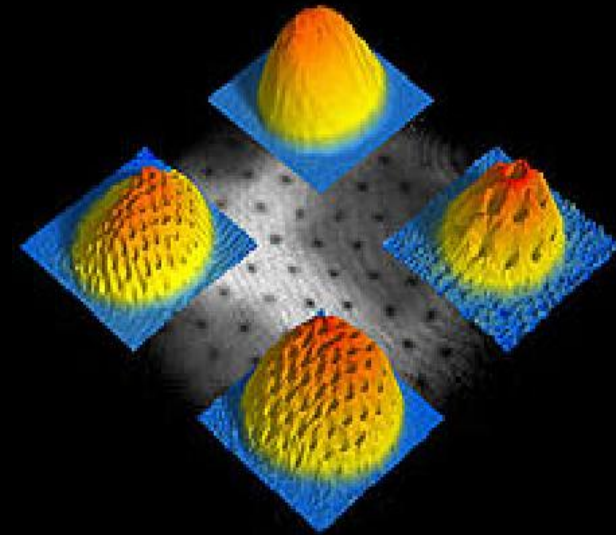


Zależna od czasu metoda funkcjonału gęstości energii – teoria i praktyka opisu dynamiki układów nadciekłych



Time=246.3



Piotr Magierski
(Politechnika Warszawska)

GOAL:

Description of fermionic superfluids (nuclei and quantum gases) far from equilibrium.

From quantum mechanics:

$$i\hbar \frac{\partial}{\partial t} \psi = \hat{H} \psi$$

*However even if we know the Hamiltonian
we cannot solve in practice the above equation*

Runge Gross mapping

$$i\hbar \frac{\partial}{\partial t} |\psi(t)\rangle = \hat{H} |\psi(t)\rangle, \quad |\psi_0\rangle = |\psi(t_0)\rangle$$

$$\frac{\partial \rho}{\partial t} + \nabla \cdot \vec{j} = 0$$

$$\left. \begin{array}{l} \rho(\vec{r}, t) \\ |\psi(t_0)\rangle \end{array} \right\} \leftrightarrow e^{i\alpha(t)} |\psi(t)\rangle$$

Up to an arbitrary function $\alpha(t)$

and consequently the functional exists:

$$F[\psi_0, \rho] = \int_{t_0}^{t_1} \langle \psi[\rho] | \left(i\hbar \frac{\partial}{\partial t} - \hat{H} \right) | \psi[\rho] \rangle dt$$

Kohn-Sham approach


Suppose we are given the density of an interacting system.
There exists a unique noninteracting system with the same density.

Interacting system

$$i\hbar \frac{\partial}{\partial t} |\psi(t)\rangle = (\hat{T} + \hat{V}(t) + \hat{W}) |\psi(t)\rangle$$

Noninteracting system

$$i\hbar \frac{\partial}{\partial t} |\varphi(t)\rangle = (\hat{T} + \hat{V}_{KS}(t)) |\varphi(t)\rangle$$


$$\rho(\vec{r}, t) = \langle \psi(t) | \hat{\rho}(\vec{r}) | \psi(t) \rangle = \langle \varphi(t) | \hat{\rho}(\vec{r}) | \varphi(t) \rangle$$

$$V_{KS}(\vec{r}, t) = \frac{\delta F[\rho]}{\delta \rho(\vec{r}, t)}$$

DFT approach is essentially exact.

Superconductivity/superfluidity in DFT

Anomalous density (superconducting order parameter):

$$v(\vec{r}, \vec{r}', t) = \langle \varphi(t) | \hat{a}_{\uparrow}(\vec{r}') \hat{a}_{\downarrow}(\vec{r}) | \varphi(t) \rangle$$

Pairing potential:

$$\Delta_{KS}(\vec{r}, \vec{r}', t) = - \frac{\delta F[\rho, \chi]}{\delta v^*(\vec{r}, \vec{r}', t)}$$

L.N. Oliveira, E.K.U. Gross, W. Kohn, Phys. Rev. Lett. 60 2430 (1988)

O.J. Wacker, R. Kummel, E.K.U. Gross, Phys. Rev. Lett. 73 2915 (1993)

For nonlocal pairing potential the resulting equations are integro-differential equations in coordinate space.

SLDA - Extension of Kohn-Sham approach to superfluid Fermi systems

$$E_{gs} = \int d^3r \varepsilon(n(\vec{r}), \tau(\vec{r}), \nu(\vec{r}))$$

$$n(\vec{r}) = 2 \sum_k |\mathbf{v}_k(\vec{r})|^2, \quad \tau(\vec{r}) = 2 \sum_k |\vec{\nabla} \mathbf{v}_k(\vec{r})|^2$$

$$\nu(\vec{r}) = \sum_k \mathbf{u}_k(\vec{r}) \mathbf{v}_k^*(\vec{r}) \quad \leftarrow \text{pairing (anomalous) density}$$

$$\begin{pmatrix} T + U(\vec{r}) - \mu & \Delta(\vec{r}) \\ \Delta^*(\vec{r}) & -(T + U(\vec{r}) - \mu) \end{pmatrix} \begin{pmatrix} \mathbf{u}_k(\vec{r}) \\ \mathbf{v}_k(\vec{r}) \end{pmatrix} = E_k \begin{pmatrix} \mathbf{u}_k(\vec{r}) \\ \mathbf{v}_k(\vec{r}) \end{pmatrix}$$

Mean-field and pairing field are both local fields!

(for sake of simplicity spin degrees of freedom are not shown)

There is a problem!
The pairing field diverges.

One has to introduce position and momentum dependent running coupling constant.

Bulgac, Yu, Phys. Rev. Lett. 88 (2002) 042504
Bulgac, Phys. Rev. C65 (2002) 051305

$$\begin{cases} [h(\vec{r}) - \mu] u_i(\vec{r}) + \Delta(\vec{r}) v_i(\vec{r}) = E_i u_i(\vec{r}) \\ \Delta^*(\vec{r}) u_i(\vec{r}) - [h(\vec{r}) - \mu] v_i(\vec{r}) = E_i v_i(\vec{r}) \end{cases} \quad \begin{cases} h(\vec{r}) = -\vec{\nabla} \frac{\hbar^2}{2m(\vec{r})} \vec{\nabla} + U(\vec{r}) \\ \Delta(\vec{r}) = -g_{\text{eff}}(\vec{r}) \nu_c(\vec{r}) \end{cases}$$

$$\frac{1}{g_{\text{eff}}(\vec{r})} = \frac{1}{g[n(\vec{r})]} - \frac{m(\vec{r}) k_c(\vec{r})}{2\pi^2 \hbar^2} \left\{ 1 - \frac{k_F(\vec{r})}{2k_c(\vec{r})} \ln \frac{k_c(\vec{r}) + k_F(\vec{r})}{k_c(\vec{r}) - k_F(\vec{r})} \right\}$$

$$\rho_c(\vec{r}) = 2 \sum_{E_i \geq 0} |\mathbf{v}_i(\vec{r})|^2, \quad \nu_c(\vec{r}) = \sum_{E_i \geq 0} \mathbf{v}_i^*(\vec{r}) \mathbf{u}_i(\vec{r})$$

$$E_c + \mu = \frac{\hbar^2 k_c^2(\vec{r})}{2m(\vec{r})} + U(\vec{r}), \quad \mu = \frac{\hbar^2 k_F^2(\vec{r})}{2m(\vec{r})} + U(\vec{r})$$

Formalism for Time Dependent Phenomena: TDSLDA

A.K. Rajagopal and J. Callaway, Phys. Rev. B **7**, 1912 (1973)
 V. Peuckert, J. Phys. C **11**, 4945 (1978)
 E. Runge and E.K.U. Gross, Phys. Rev. Lett. **52**, 997 (1984)

Local density approximation (no memory effects – adiabatic TDDFT)

$$i\hbar \frac{\partial}{\partial t} \begin{pmatrix} u_{k\uparrow}(\mathbf{r}, t) \\ u_{k\downarrow}(\mathbf{r}, t) \\ v_{k\uparrow}(\mathbf{r}, t) \\ v_{k\downarrow}(\mathbf{r}, t) \end{pmatrix} = \begin{pmatrix} h_{\uparrow,\uparrow}(\mathbf{r}, t) & h_{\uparrow,\downarrow}(\mathbf{r}, t) & 0 & \Delta(\mathbf{r}, t) \\ h_{\downarrow,\uparrow}(\mathbf{r}, t) & h_{\downarrow,\downarrow}(\mathbf{r}, t) & -\Delta(\mathbf{r}, t) & 0 \\ 0 & -\Delta^*(\mathbf{r}, t) & -h_{\uparrow,\uparrow}^*(\mathbf{r}, t) & -h_{\uparrow,\downarrow}^*(\mathbf{r}, t) \\ \Delta^*(\mathbf{r}, t) & 0 & -h_{\downarrow,\uparrow}^*(\mathbf{r}, t) & -h_{\downarrow,\downarrow}^*(\mathbf{r}, t) \end{pmatrix} \begin{pmatrix} u_{k\uparrow}(\mathbf{r}, t) \\ u_{k\downarrow}(\mathbf{r}, t) \\ v_{k\uparrow}(\mathbf{r}, t) \\ v_{k\downarrow}(\mathbf{r}, t) \end{pmatrix}$$

Density functional contains normal densities, anomalous density (pairing) and currents:

$$E(t) = \int d^3r \left[\varepsilon(n(\vec{r}, t), \tau(\vec{r}, t), \nu(\vec{r}, t), \vec{j}(\vec{r}, t)) + V_{ext}(\vec{r}, t)n(\vec{r}, t) + \dots \right]$$

Density
functional for
unitary Fermi
gas

Nuclear energy
functional: Sly4,
SkP, SkM*, ...

TDSLDA is formulated on the 3D lattice without any symmetry restrictions.
 Initial conditions for TDSLDA are generated through adiabatic switching and quantum friction.
Important: one has to evolve all „single-particle“ states!

Advantages of TDDFT

- 1) Usually less complicated than other approaches.
- 2) The same framework describes various limits: eg. linear and highly nonlinear regimes.
- 1) Uses space-time variables for which we have better intuition than eg. in case of energy representation.
- 4) The simulation follow closely the way how the experiments are conducted.

Typical procedure:

- prepare the initial state of the system (usually the ground state of nucleus/nuclei) using static DFT.
- start evolution: either by applying external field (e.g. simulating photon absorption) or making nuclei to move against each other (phase change of orbitals)
- evolve the system to desired final time
- at each selected time one can extract interesting physical quantities

Some other advantages:

- TDDFT does not require introduction of hard-to-define collective degrees of freedom and there are no ambiguities arising from defining potential energy surfaces (PES) and inertias.
- Interaction with basically any external probe (weak or strong) easy to implement.
- In principle it offers a consistent way to reconstruct the energy spectrum through re-quantization of TDDFT trajectories (No need for considering off-diagonal matrix elements which have vague meaning in the DFT framework)

Challenges of TDDFT

1) There are easy and difficult observables in DFT.

In general: easy observables are one-body observables. They are easily extracted and reliable.

2) But there are also important observables which are difficult to extract.

For example:

- S matrix (important for scattering):

$$S_{fi} = \lim_{t \rightarrow \infty} \langle \Phi_f | \Phi(t) \rangle; \quad \lim_{t \rightarrow -\infty} |\Phi(t)\rangle = |\Phi_i\rangle$$

- momentum distributions

- transitional densities (defined in linear response regime)

- various conditional probabilities.

3) Memory effects.

In general the evolution of the system in TDDFT will depend on the past.

Very little is known about the memory terms, but in principle it can be long ranged (see eg. Dobson, Brunner, Gross, Phys. Rev. Lett. 79 (1997) 1905)

Memory effects are usually neglected = adiabatic approximation

Result: dissipation effects are not correctly taken into account except for one-body dissipation

Single particle potential (Skyrme):

$$h(\mathbf{r}) = -\vec{\nabla} \cdot \left(B(\mathbf{r}) + \vec{\sigma} \cdot \vec{C}(\mathbf{r}) \right) \vec{\nabla} + U(\mathbf{r}) + \frac{1}{2i} \left[\vec{W}(\mathbf{r}) \cdot (\vec{\nabla} \times \vec{\sigma}) + \vec{\nabla} \cdot (\vec{\sigma} \times \vec{W}(\mathbf{r})) \right] \\ + \vec{U}_\sigma(\mathbf{r}) \cdot \vec{\sigma} + \frac{1}{i} \left(\vec{\nabla} \cdot \vec{U}_\Delta(\mathbf{r}) + \vec{U}_\Delta(\mathbf{r}) \cdot \vec{\nabla} \right)$$

where

$$\begin{aligned} B(\mathbf{r}) &= \frac{\hbar^2}{2m} + C^\tau \rho \\ \vec{C}(\mathbf{r}) &= C^{sT} \vec{s} \\ U(\mathbf{r}) &= 2C^\rho \rho + 2C^{\Delta\rho} \nabla^2 \rho + C^\tau \tau + C^{\nabla J} \vec{\nabla} \cdot \vec{J} + C^\gamma (\gamma + 2) \rho^{\gamma+1} \\ \vec{W}(\mathbf{r}) &= -C^{\nabla J} \vec{\nabla} \rho \\ \vec{U}_\sigma(\mathbf{r}) &= 2C^s \vec{s} + 2C^{\Delta s} \nabla^2 \vec{s} + C^{sT} \vec{T} + C^{\nabla J} \vec{\nabla} \times \vec{j} \\ \vec{U}_\Delta(\mathbf{r}) &= C^j \vec{j} + \frac{1}{2} C^{\nabla j} \vec{\nabla} \times \vec{s} \end{aligned}$$

and pairing potential:

$$\Delta(\mathbf{r}, t) = -g_{eff}(\mathbf{r}) \chi(\mathbf{r}, t)$$

Selected capabilities of the SLDA/TDSLDA codes:

- ✓ full 3D simulations with no symmetry restrictions
- ✓ number of evolved quasiparticle wave functions is of the order of the lattice size: $O(10^4)$ - $O(10^6)$
- ✓ high numerical accuracy for spatial derivatives using FFTW
- ✓ for TD high-accuracy and numerically stable Adams–Bashforth–Milne 5th order predictor-corrector-modifier algorithm with only 2 evaluations of the rhs per time step and with no matrix operations
- ✓ Eg. we evolve $4 \times 136626 = 546504$ coupled eigenvectors for ^{238}U on the lattice: $50 \times 50 \times 80$ fm (mesh size: 1.25fm) with energy cutoff 100MeV to an accuracy 10^{-8}
- ✓ volumes of the order of ($L = 80^3$) capable of simulating time evolution of 42000 neutrons at saturation density (possible application: neutron stars)
- ✓ capable of simulating up to times of the order of 10^{-19} s (a few million time steps)
- ✓ CPU vs GPU on Titan \approx 15 speed-up (likely an additional factor of 4 possible)

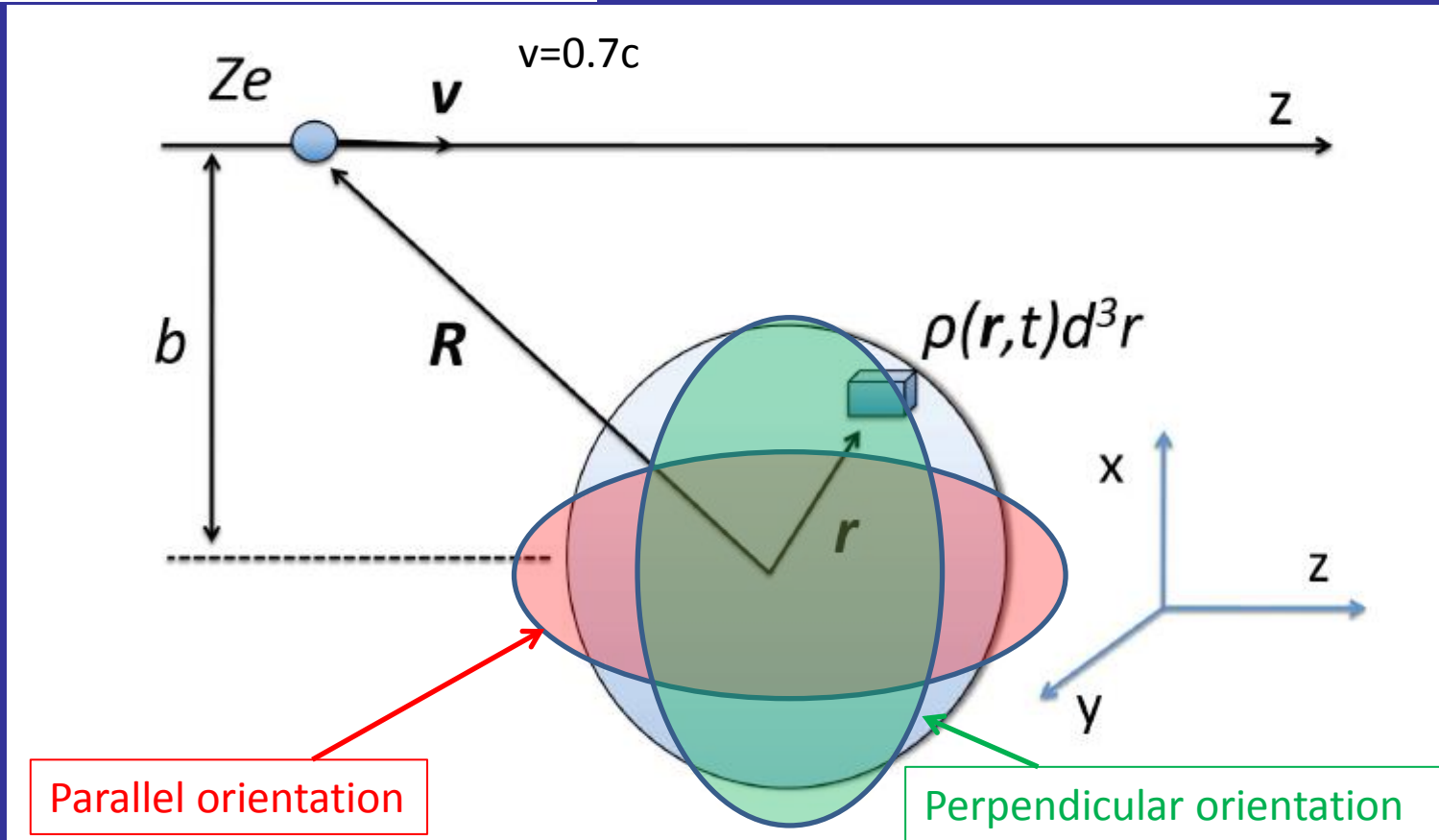
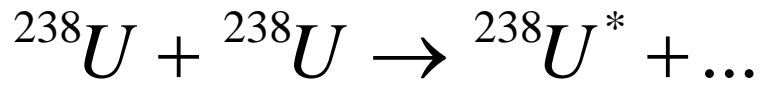
Eg. for 137062 two component wave functions:

CPU version (4096 nodes x 16 PEs) - 27.90 sec for 10 time steps

GPU version (4096 PEs + 4096GPU) - 1.84 sec for 10 time steps



Relativistic Coulomb excitation

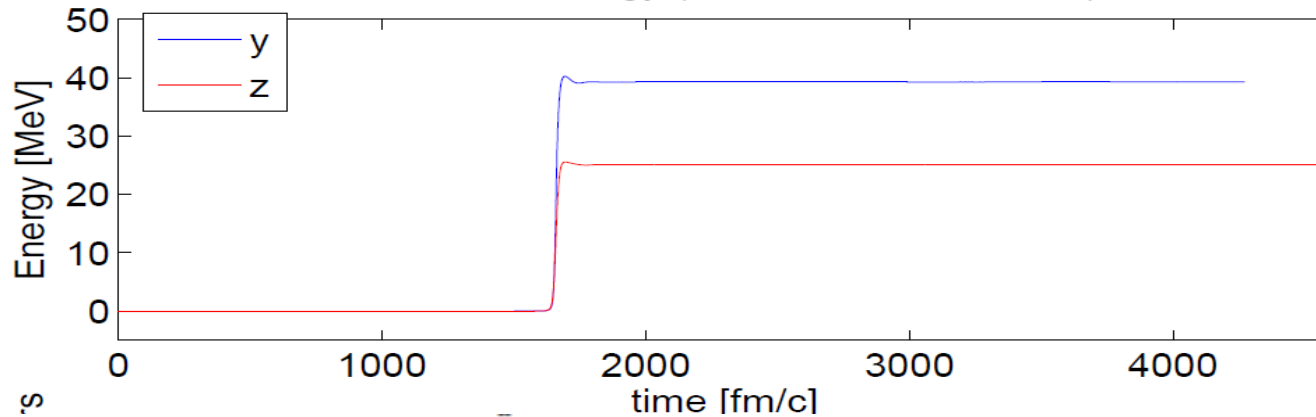


- Projectile is treated classically (its de Broglie wavelength is of the order of 0.01 fm)
- Extreme forward scattering: no deflection of the projectile
- Since we want to excite high energy modes (i.e. couple of tens of MeV) the projectile has to be relativistic:

$$\hbar\omega \approx \frac{\hbar}{\tau_{\text{coll}}} = \frac{\gamma v}{b} \approx 12 \text{ MeV} ; \gamma = \frac{1}{\sqrt{1 - (v/c)^2}}$$

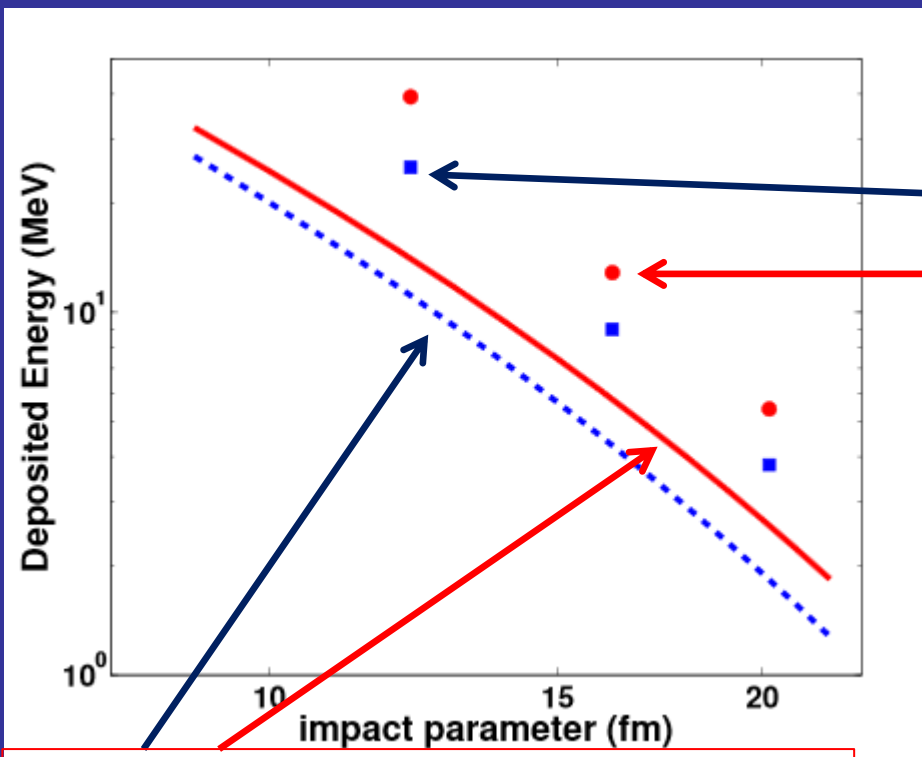
**Energy deposited for two nuclear orientations (y – perpendicular, z – parallel)
Impact parameter $b=12.2\text{fm}$**

Excitation energy (CM motion subtracted)



$b(\text{fm})$	E_{int}	E_{int}/E	E_{γ}^{int}	$E_{\gamma}^{int}/E_{\gamma}$	E_{GT}	E_{GT}^*
12.2 \perp	39.29	0.668	0.911	0.960	17.58	24.68
14.6 \perp	19.2	0.608	0.567	0.963	10.32	14.51
16.2 \perp	12.87	0.547	0.411	0.963	7.41	10.43
20.2 \perp	5.41	0.444	0.199	0.961	3.43	4.84
12.2	25.11	0.588	0.5	0.941	12.94	18.17
14.6	13.16	0.498	0.306	0.942	7.22	10.16
16.2	8.97	0.470	0.217	0.939	5.02	7.07
20.2	3.8	0.367	0.106	0.934	2.16	3.05
12.2 $\perp\perp$	24.21	0.591	0.407	0.930	12.36	17.33
14.6 $\perp\perp$	12.58	0.513	0.245	0.929	6.65	9.34
16.2 $\perp\perp$	8.5	0.464	0.175	0.926	4.49	6.32
20.2 $\perp\perp$	3.5	0.353	0.085	0.919	1.78	2.51

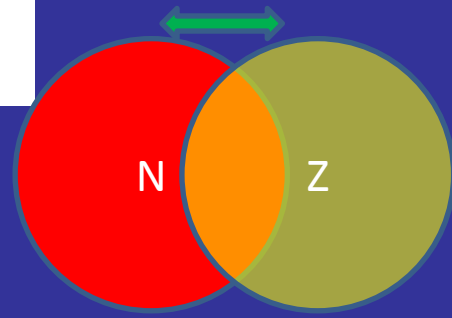
Energy transferred to the target nucleus in the form of internal excitations



TDSLDA – parallel orientation

TDSLDA – perpendicular orientation

Goldhaber-Teller like model:
proton and neutron density distributions
oscillating against each other



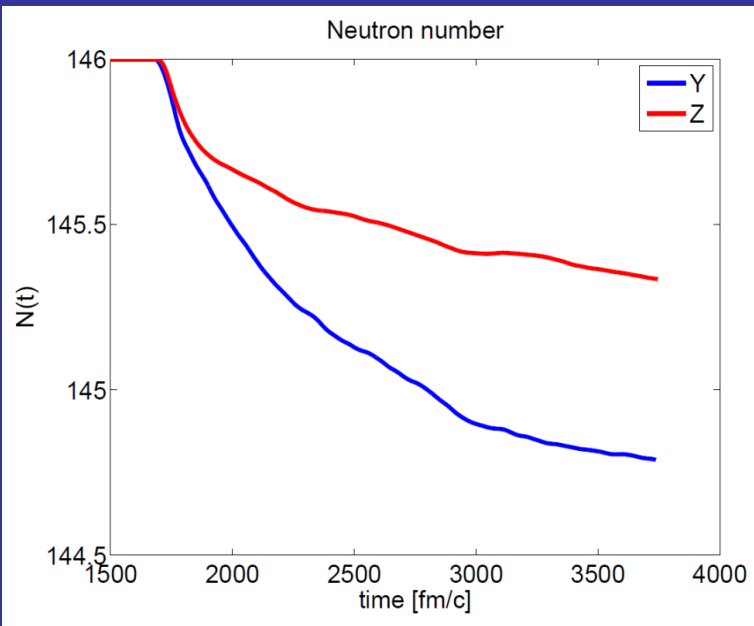
Two characteristic frequencies

$$\hbar\omega_1 = 12\text{MeV}$$
$$\hbar\omega_2 = 16\text{MeV}$$

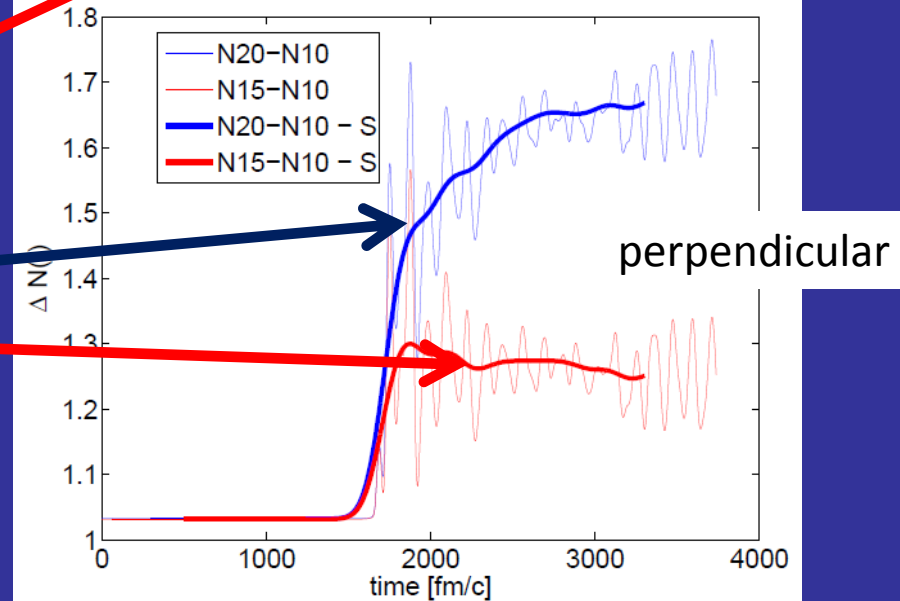
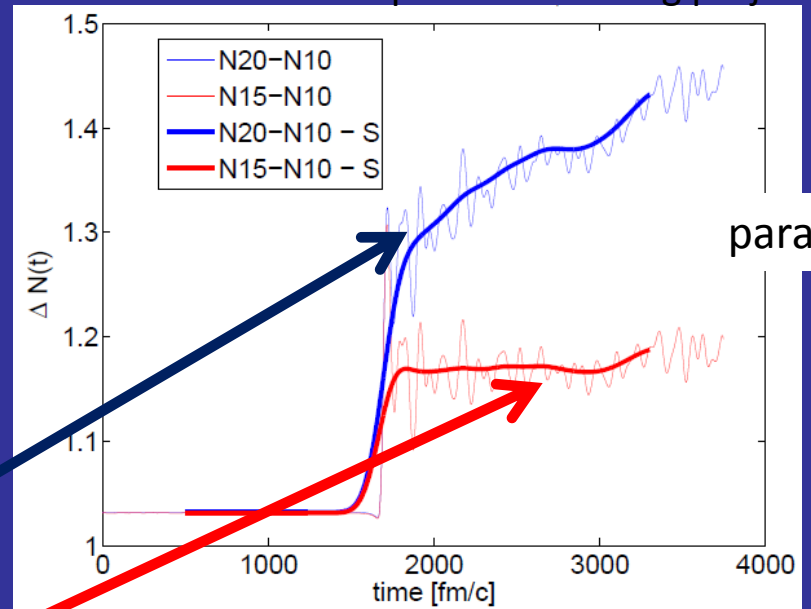
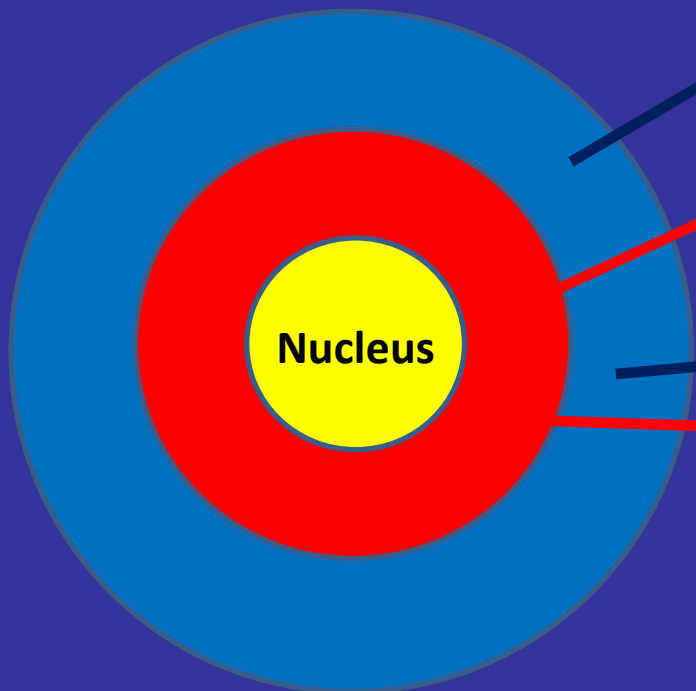
Part of the energy is transferred
to other degrees of freedom
than pure dipole moment oscillations.

Neutron emission

Impact parameter $b=12.2\text{fm}$



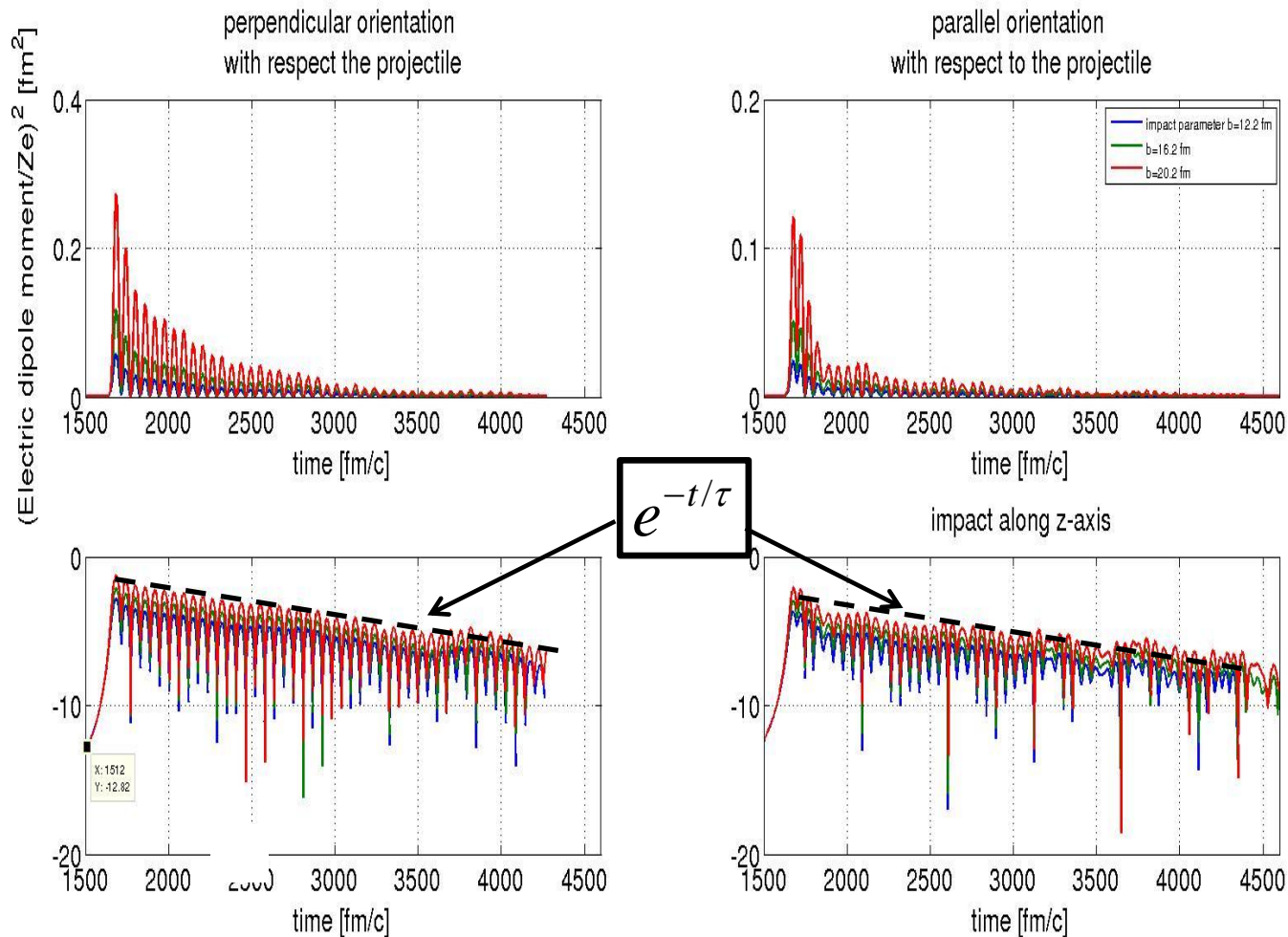
Number of neutrons in two shells surrounding nucleus for two nuclear orientations with respect to incoming projectile:



One body dissipation

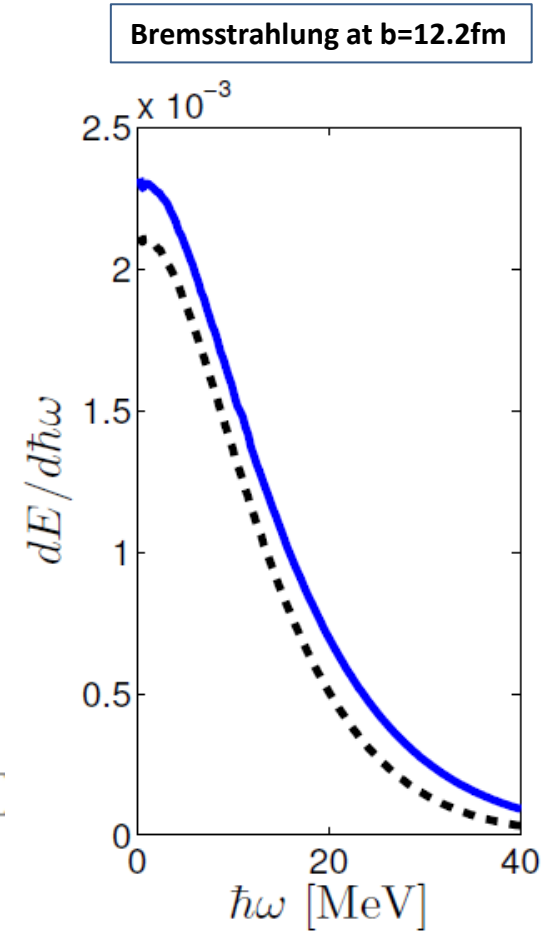
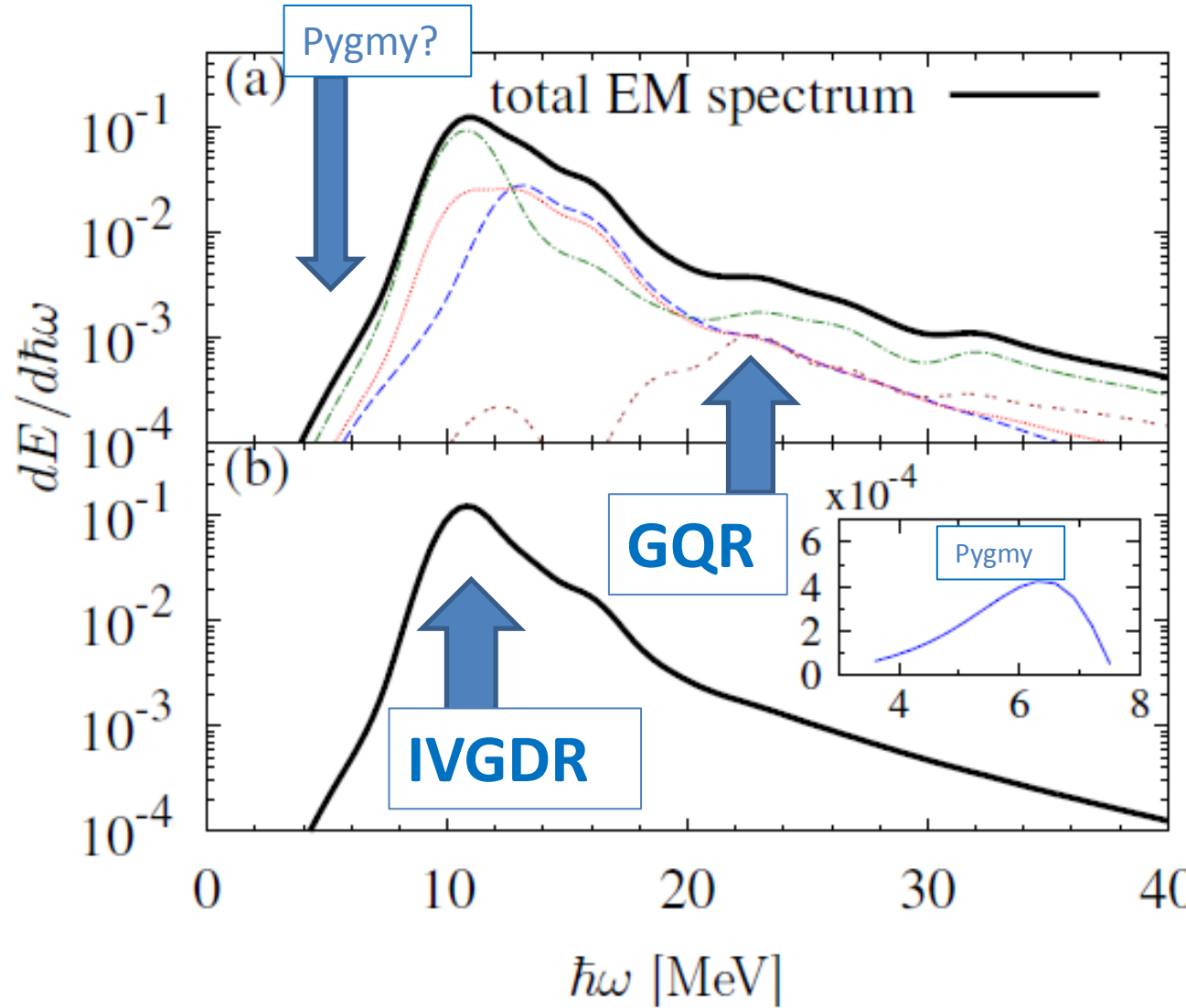
Let us assume that the collective energy of dipole oscillation is proportional the square of the amplitude of electric dipole moment:

$$E_{coll}(t) \propto [D_{max}(t)]^2$$

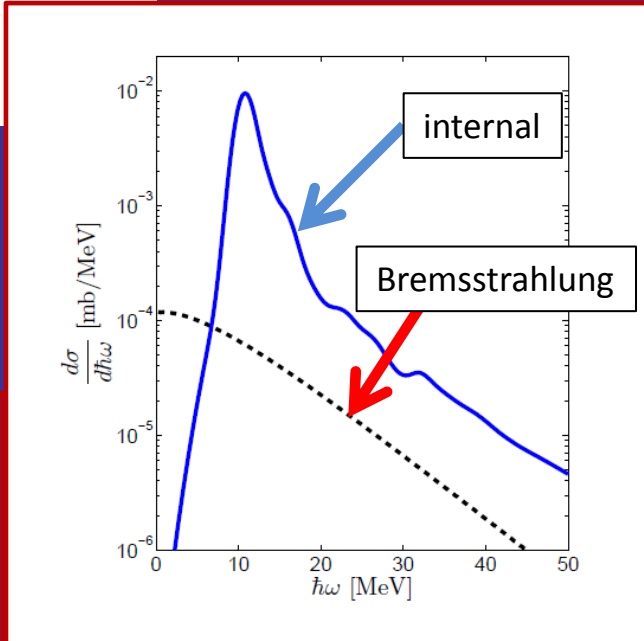
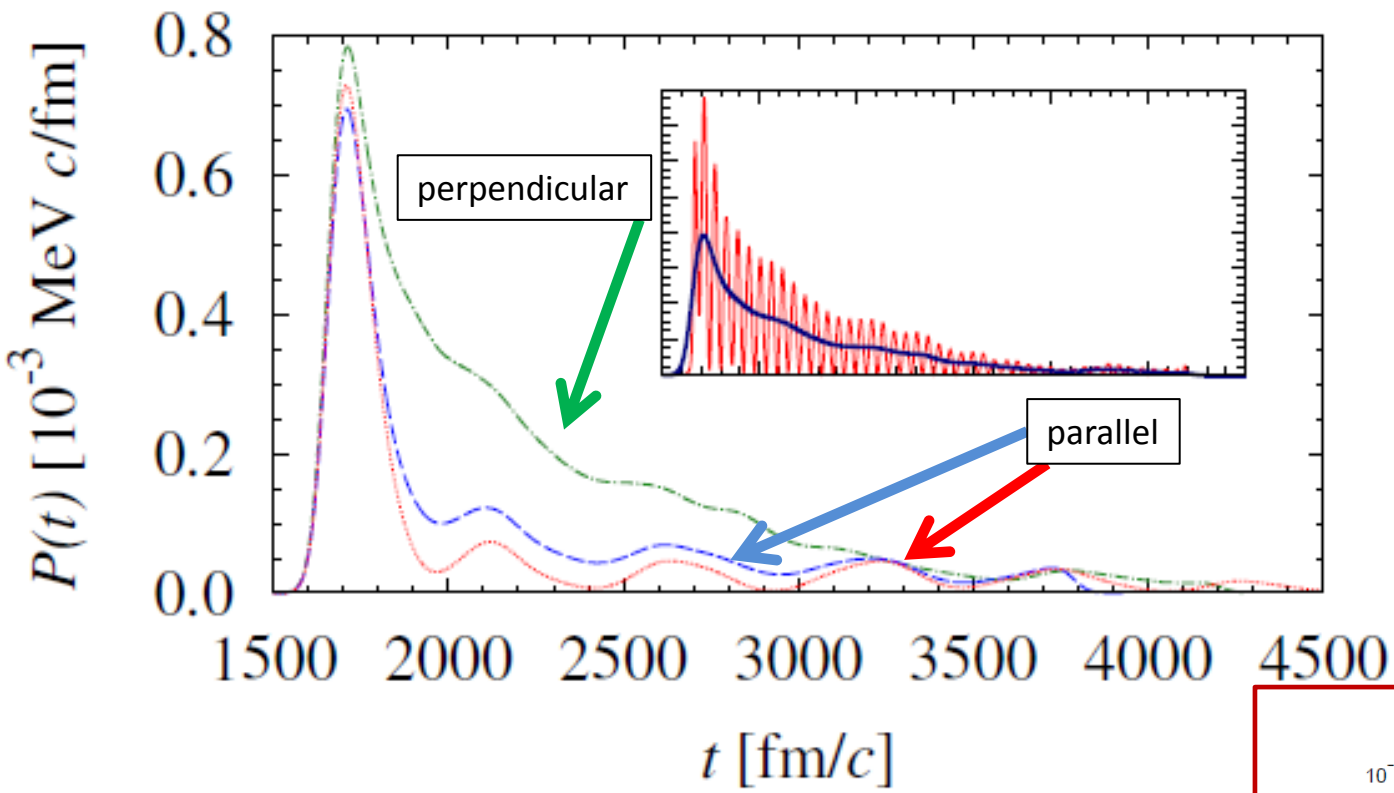


$$E_{coll}(t) \propto e^{-t/\tau}; \quad \tau \approx 500 \text{ fm} / c \Rightarrow \Gamma_{\downarrow} \approx 0.4 \text{ MeV}$$

Electromagnetic radiation due to the internal nuclear motion

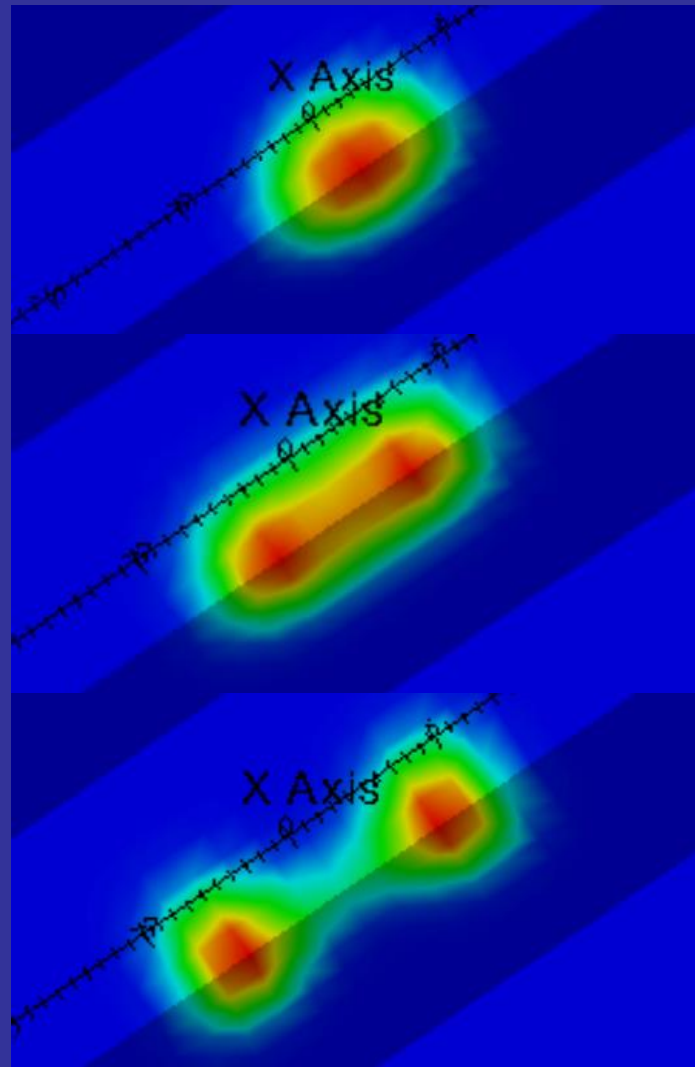


Electromagnetic radiation rate due to the internal motion



The contributions to the cross section with respect to gamma emission during 2500 fm/c after collision

Current studies: induced fission



Questions to address:

- dynamics beyond scission point.
- evolution of deformation: axial vs nonaxial.
- kinetic energy of fragments vs excitation energy.
- kinetic energy distribution of fragments.
- excitation energy of fragments (which modes?).
- neutron emission from the neck.

Toy model of ^{32}S splitting into two ^{16}O in real time at about 70 MeV excitation. Now also Pu and Fm isotopes are being considered...

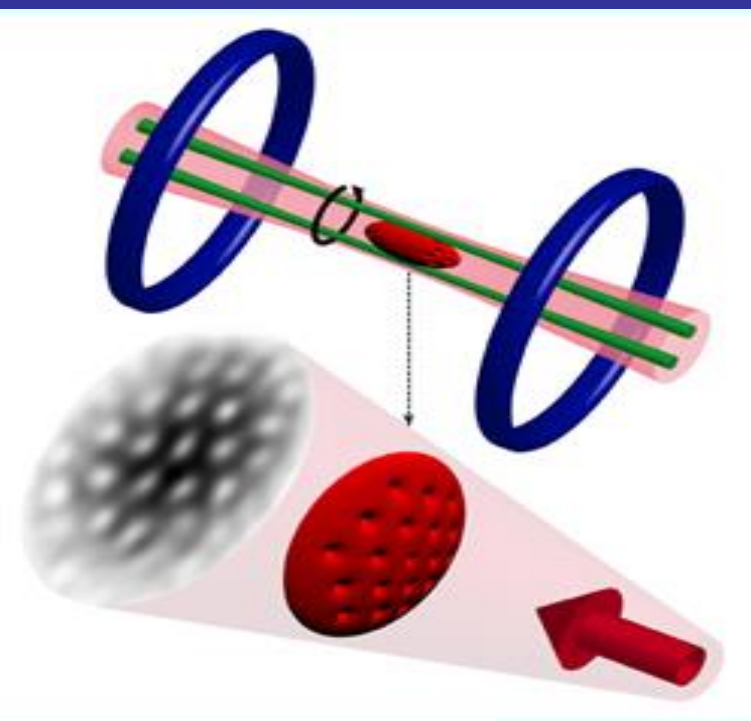
J. Grineviciute, I. Stetcu, ...

Short (selective) history:

- ✓ In 1999 DeMarco and Jin created a degenerate atomic Fermi gas.
- ✓ In 2005 Zwierlein/Ketterle group observed quantum vortices which survived when passing from BEC to unitarity - evidence for superfluidity!

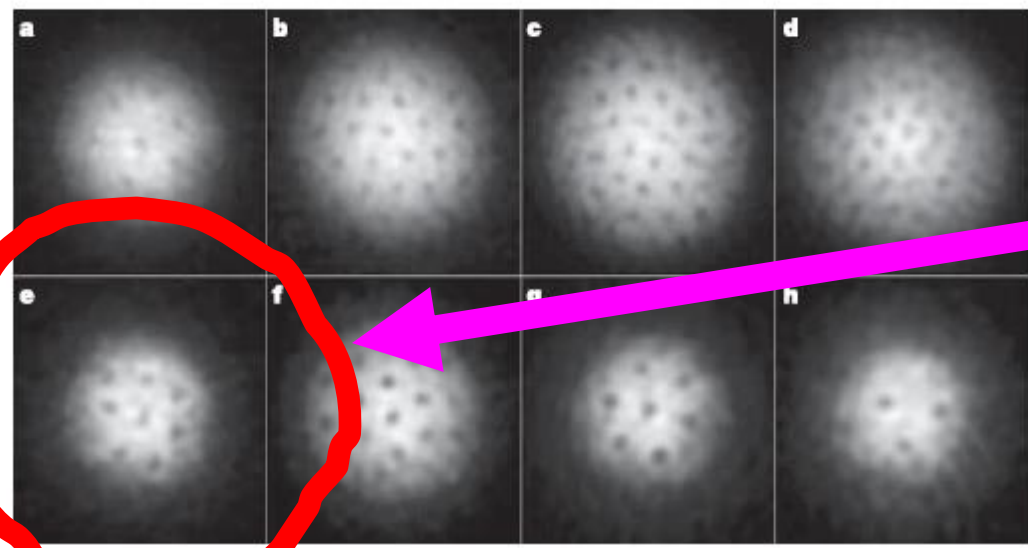
system of fermionic ${}^6\text{Li}$ atoms

Feshbach resonance:
 $B=834\text{G}$



BEC side:
 $a > 0$

BCS side:
 $a < 0$



UNITARY REGIME

Figure 2 | Vortices in a strongly interacting Fermionic atoms on the BEC- and the BCS-side of the Feshbach resonance. At the given field, the cloud of lithium atoms was stirred for 300 ms (a) or 500 ms (b-h) followed by an equilibration time of 500 ms. After 2 ms of ballistic expansion, the

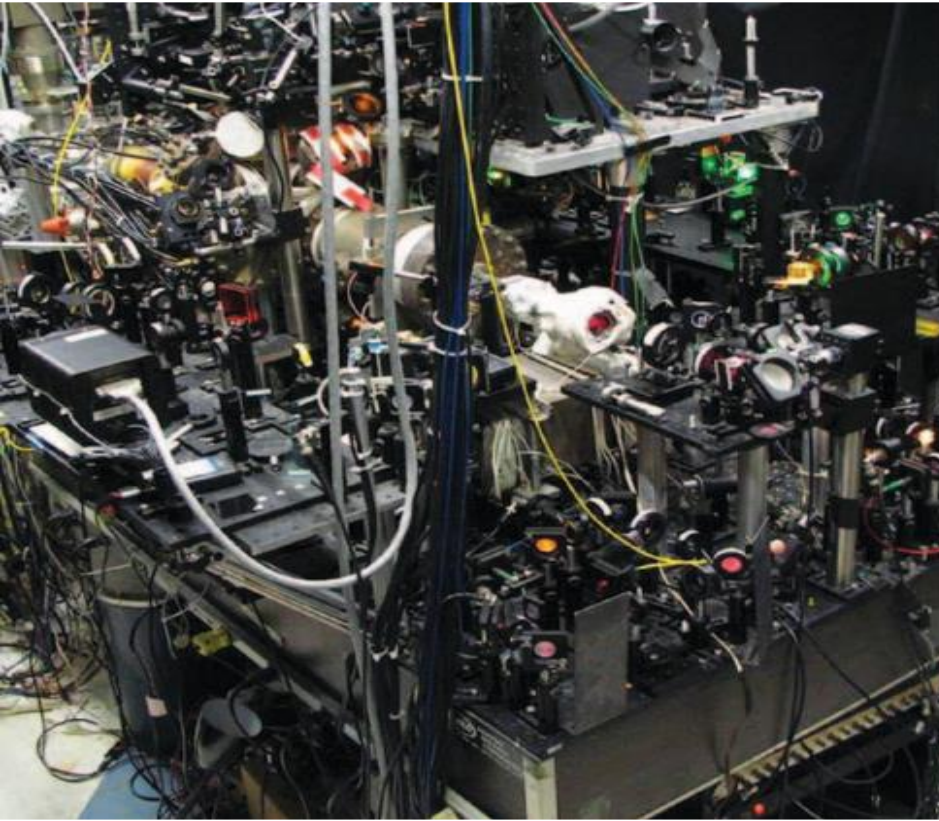
magnetic field was ramped to 735 G for imaging (see Methods). The magnetic fields were 740 G (a), 766 G (b), 792 G (c), 843 G (f), 853 G (g) and 863 G (h). The field of view is $880 \mu\text{m} \times 880 \mu\text{m}$.

M.W. Zwierlein *et al.*,
Nature, 435, 1047 (2005)

Gases of ultracold atoms and quark gluon plasma teach us how matter behaves under the strongest interactions that nature allows

Little Fermi Collider (MIT)

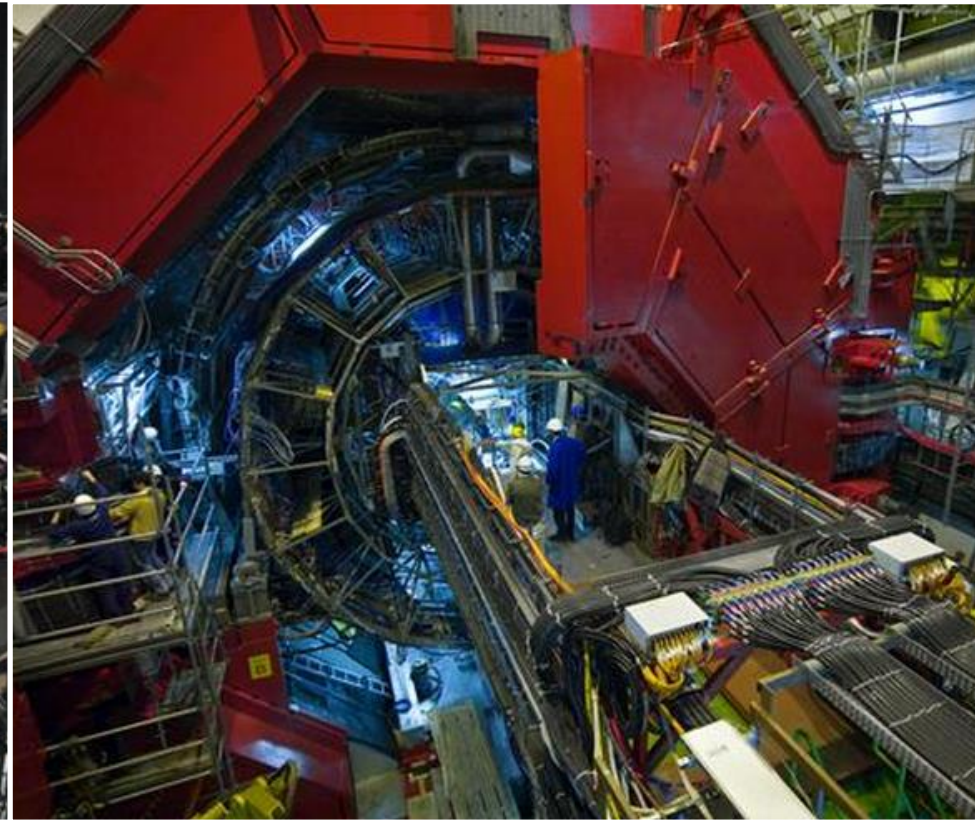
Cooling and trapping of 0.1-1 million of atoms



Vacuum chamber, countless mirrors, magnetic coils, water cooling, CCD cameras and lasers for laser cooling of atomic gases (human size)

Large Hadron Collider (CERN)

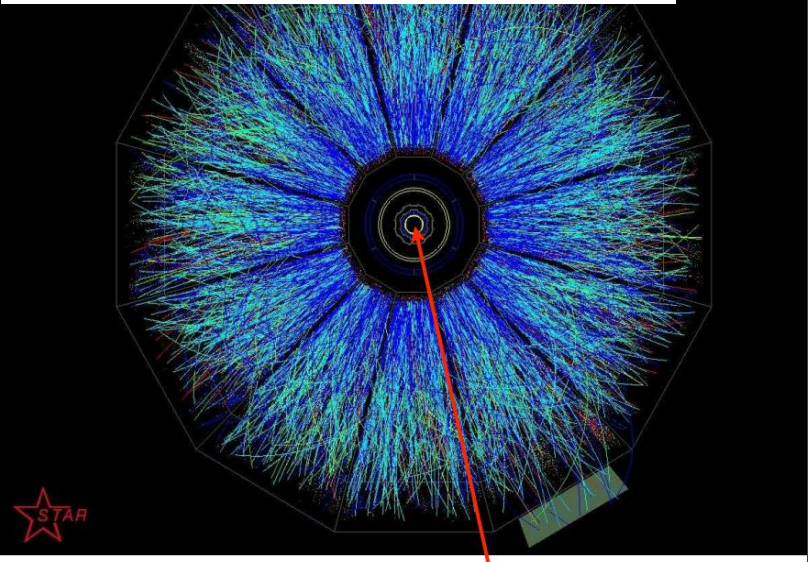
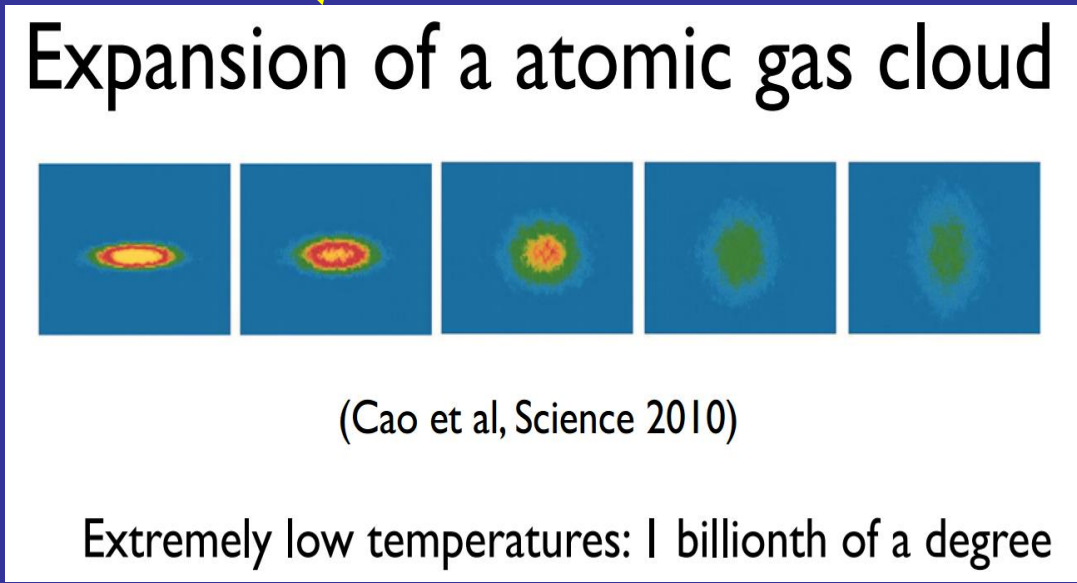
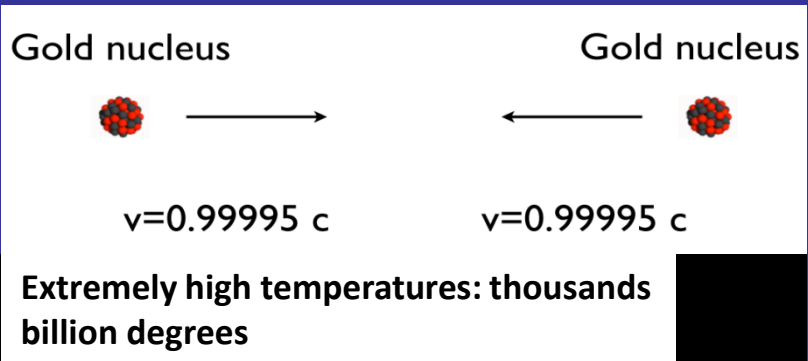
Collision of heavy nuclei in order to create quark gluon plasma



ALICE experiment: search for quark gluon plasma
view of the ALICE detector: 26m x 16m x 16 m +
particle collider in a tunnel of 27 km circumference

Perfect fluid $\frac{\eta}{S} = \frac{\hbar}{4\pi k_B}$ - strongly interacting quantum system = No well defined quasiparticles

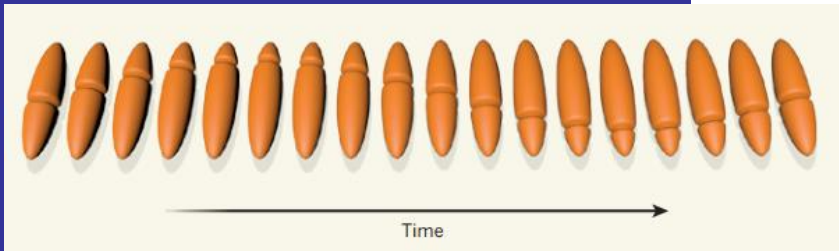
Candidates: quark gluon plasma, atomic gas



a very dense droplet of matter in the beginning

Despite of energy scales differing by many orders of magnitude, expansion of both system is pretty much similar and in particular exhibits the so-called elliptic flow.

Soliton dynamics vs ring vortex – a controversy



MIT Experiment:
Nature 499 (2013) 426

Theory prefers ring vortices:

A. Bulgac, M. M. Forbes,
M.M. Kelley, K. J. Roche, G.
Wlazłowski, Phys. Rev. Lett.
112, 025301 (2014)

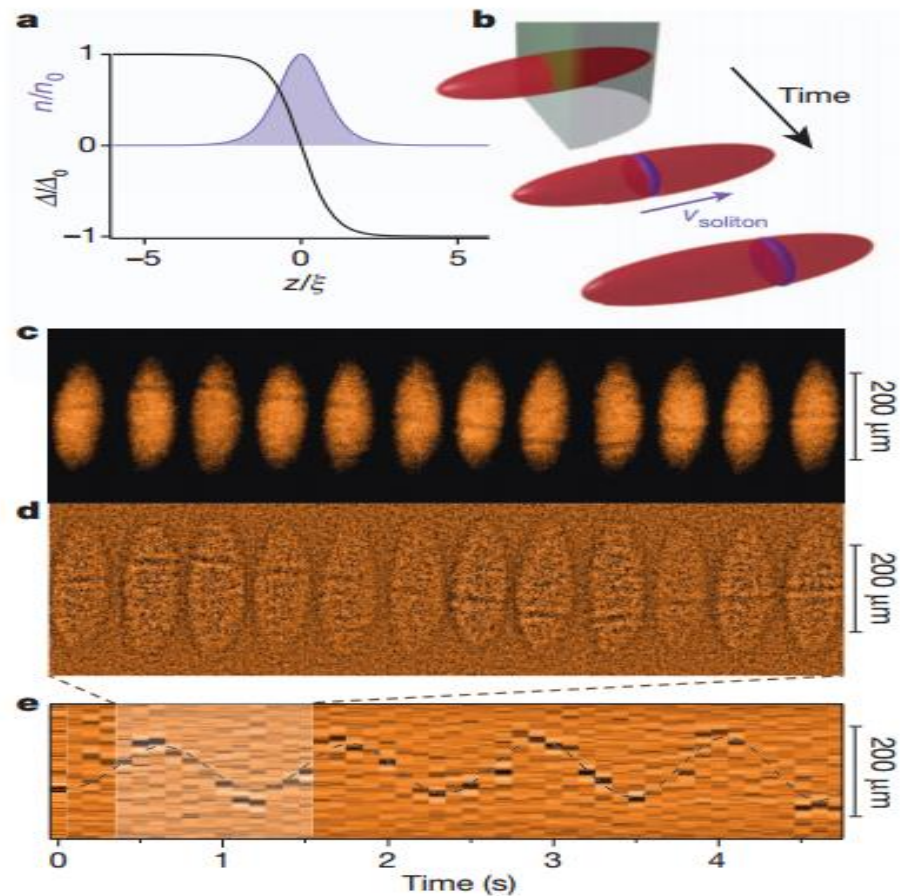


Figure 1 | Creation and observation of solitons in a fermionic superfluid. **a**, Superfluid pairing gap $\Delta(z)$ for a stationary soliton, normalized by the bulk pairing gap Δ_0 , and density $n(z)$ of the localized bosonic (fermionic) state versus position z , in the BEC (BCS) regime of the crossover, in units of the BEC healing length (BCS coherence length) ξ . **b**, Diagram of the experiment. A phase-imprinting laser beam twists the phase of one-half of the trapped superfluid by approximately π . The soliton generally moves at non-zero velocity v_{soliton} . **c**, Optical density and **d**, residuals (optical density minus a smoothed copy of the same image) of atom clouds at 815 G, imaged via the rapid ramp method³⁴, showing solitons at various hold times after creation. One period of soliton oscillation is shown. The in-trap aspect ratio was $\lambda = 6.5(1)$. **e**, Radially integrated residuals as a function of time revealing long-lived soliton oscillations. The soliton period is $T_s = 12(2)T_z$, much longer than the trapping period of $T_z = 93.76(5)$ ms, revealing an extreme enhancement of the soliton's relative effective mass, M^*/M .

Road to quantum turbulence

Classical turbulence: energy is transferred from large scales to small scales where it eventually dissipates.

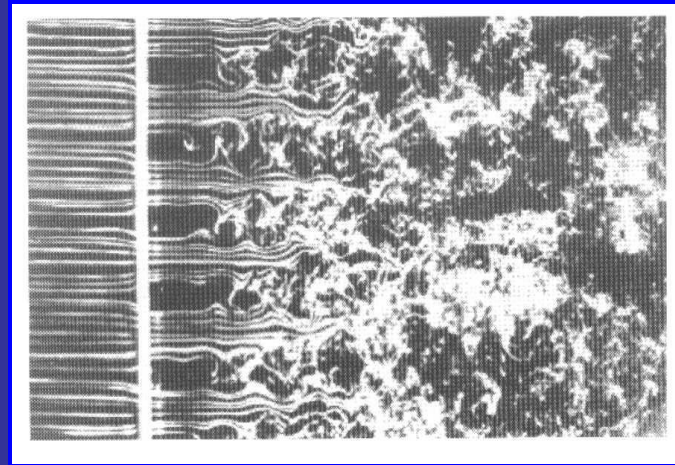
Kolmogorov spectrum: $E(k) = C \varepsilon^{2/3} k^{-5/3}$

E – kinetic energy per unit mass associated with the scale $1/k$

ε - energy rate (per unit mass) transferred to the system at large scales.

k - wave number (from Fourier transformation of the velocity field).

C – dimensionless constant.



Superfluid turbulence (quantum turbulence): disordered set of quantized vortices. The friction between the superfluid and normal part of the fluid serves as a source of energy dissipation.

Problem: how the energy is dissipated in the superfluid system at small scales at $T=0$? - „pure“ quantum turbulence

Possibility: vortex reconnections \rightarrow Kelvin waves \rightarrow phonon radiation

Road to quantum turbulence

Classical turbulence: energy is transferred from large scales to small scales where it eventually dissipates.

Kolmogorov spectrum: $E(k) = C \varepsilon^{2/3} k^{-5/3}$

E – kinetic energy per unit mass associated with the scale $1/k$

ε - energy rate (per unit mass) transferred to the system at large scales.

k - wave number (from Fourier transformation of the velocity field).

C – dimensionless constant.

Superfluid turbulence (quantum turbulence): disordered set of quantized vortices. The friction between the superfluid and normal part of the fluid serves as a source of energy dissipation.

Problem: how the energy is dissipated in the superfluid system at small scales at $T=0$? - „pure“ quantum turbulence

Possibility: vortex reconnections \rightarrow Kelvin waves \rightarrow phonon radiation

From fully microscopic small scale simulations:

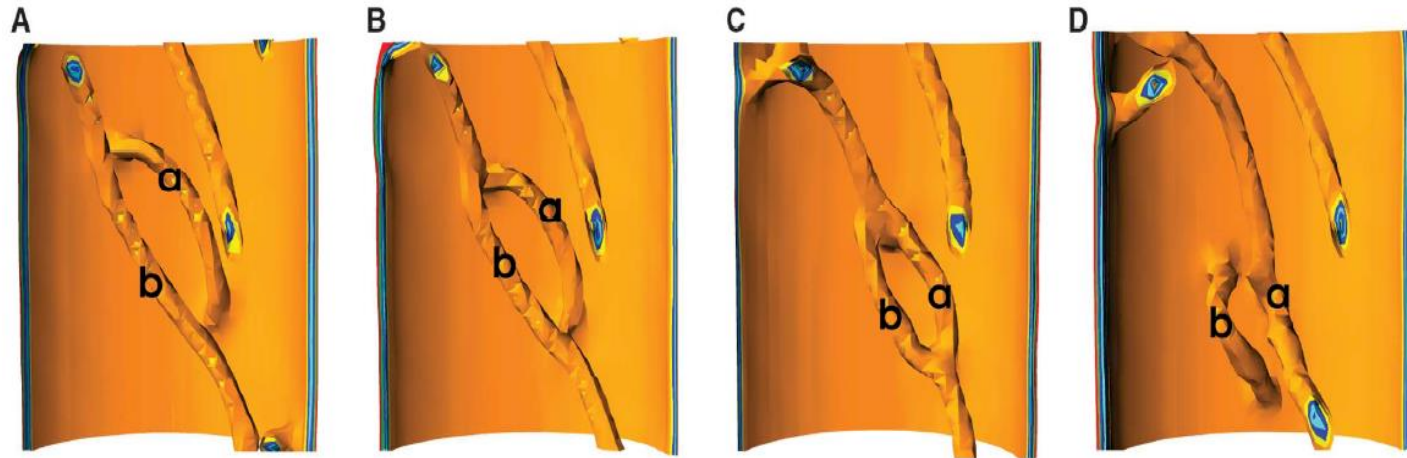
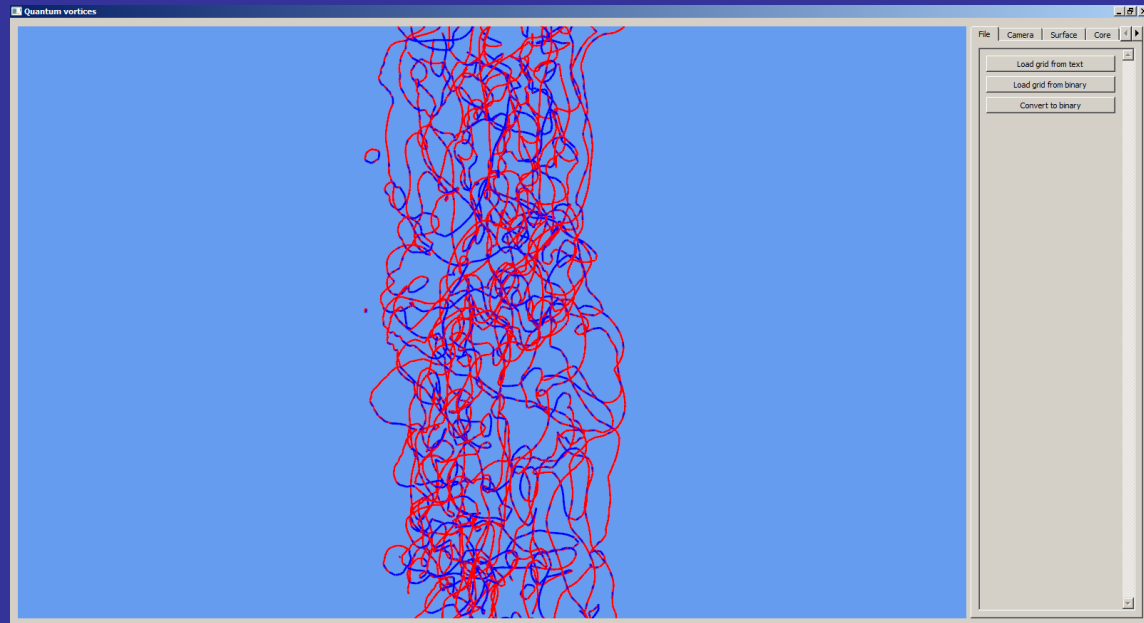


Fig. 3. (A to D) Two vortex lines approach each other, connect at two points, form a ring and exchange between them a portion of the vortex line, and subsequently separate. Segment (a), which initially belonged to the vortex line attached to the wall, is transferred to the long vortex line (b) after reconnection and vice versa.

Bulgac, Luo, Magierski, Roche, Yu, *Science* 332, 1288 (2011)

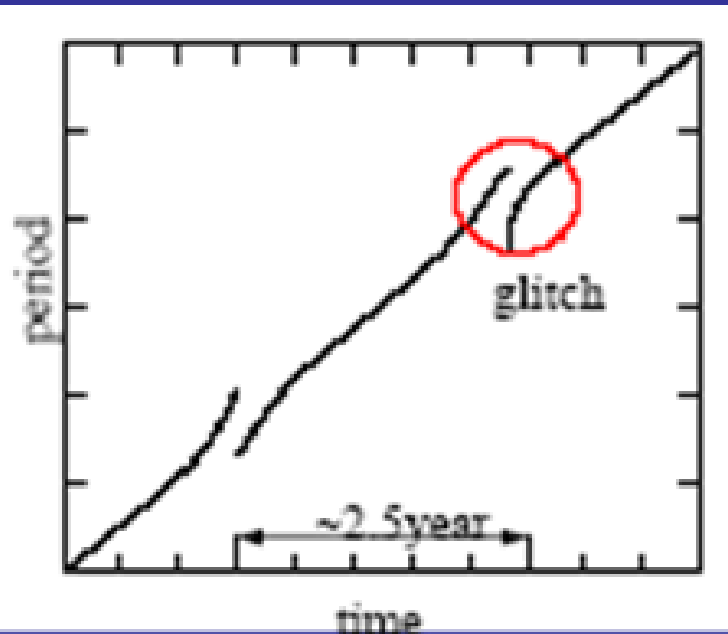
to large scale calculations
(using simplified approach
based on GPE-type eq. but
consistent with TDSLDA):

Magierski, Wlazłowski, Stefko
vortex analysis: Porter-Sobieraj, Bączyk



Another application: dynamics of neutron stars

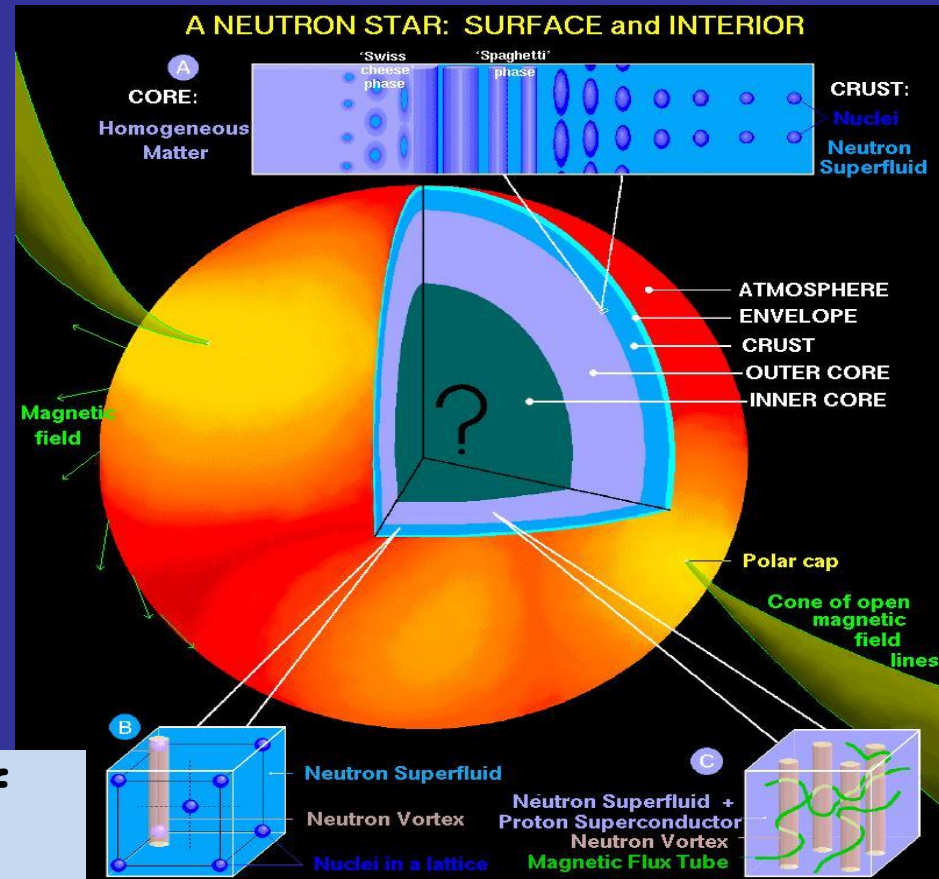
Neutron star is a huge superfluid



glitch phenomenon = a sudden speed up of rotation.

To date more than 300 glitches have been detected in more than 100 pulsars

Glitch phenomenon is commonly believed to be related to rearrangement of vortices in the interior of neutron stars. It would require however a correlated behavior of huge number of quantum vortices and the mechanism of such collective rearrangement is still a mystery.



TDSLDA applications:

1) Nuclear physics:

- Electromagnetic response
- Pairing vibrations
- Heavy ion collisions
- Induced fission
- Neutron scattering/capture

2) Neutron stars:

- Dynamics of vortices
- Vortex pinning mechanism in the neutron star crust (glitches)

3) Various applications in cold atom physics.

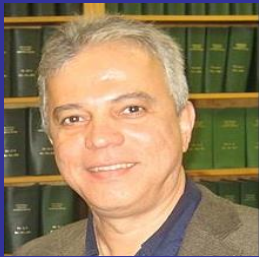
Collaborators:



Aurel Bulgac
(U. Washington)



Kenneth J. Roche
(PNNL)



Carlos Bertulani
(Texas A & M U.)



Ionel Stetcu
(LANL)



Michael M. Forbes
(WSU)

Group at Warsaw University of Technology



Gabriel Wlazłowski



Kazuyuki Sekizawa -
postdoc



Janina Grineviciute - postdoc

Computer (GPU) code optimization:

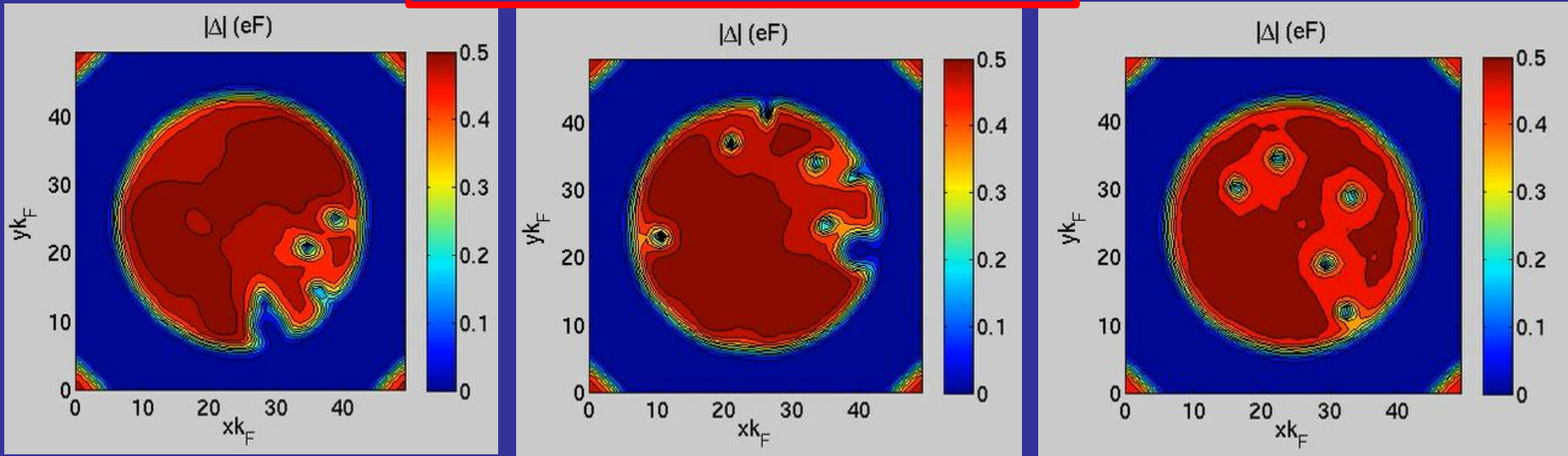
dr Witold Rudnicki (ICM)

dr Franciszek Rakowski (ICM)

Numerical data analysis:

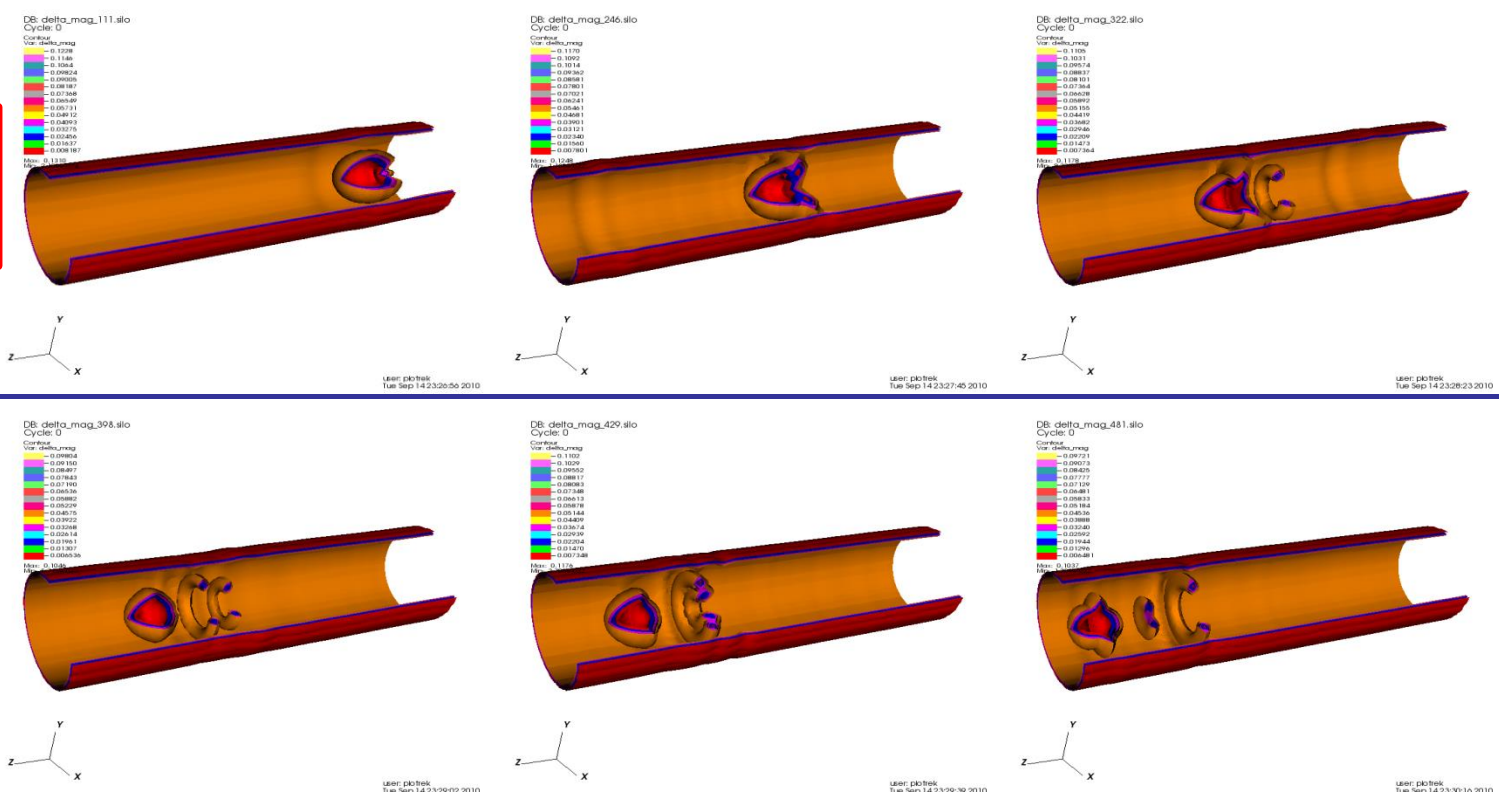
dr Joanna Porter-Sobieraj (Mathematics and Information Science, WUT)

Excitation of vortices through stirring



dynamics of vortex rings

Heavy spherical object moving through the superfluid unitary Fermi gas



Vortex reconnections

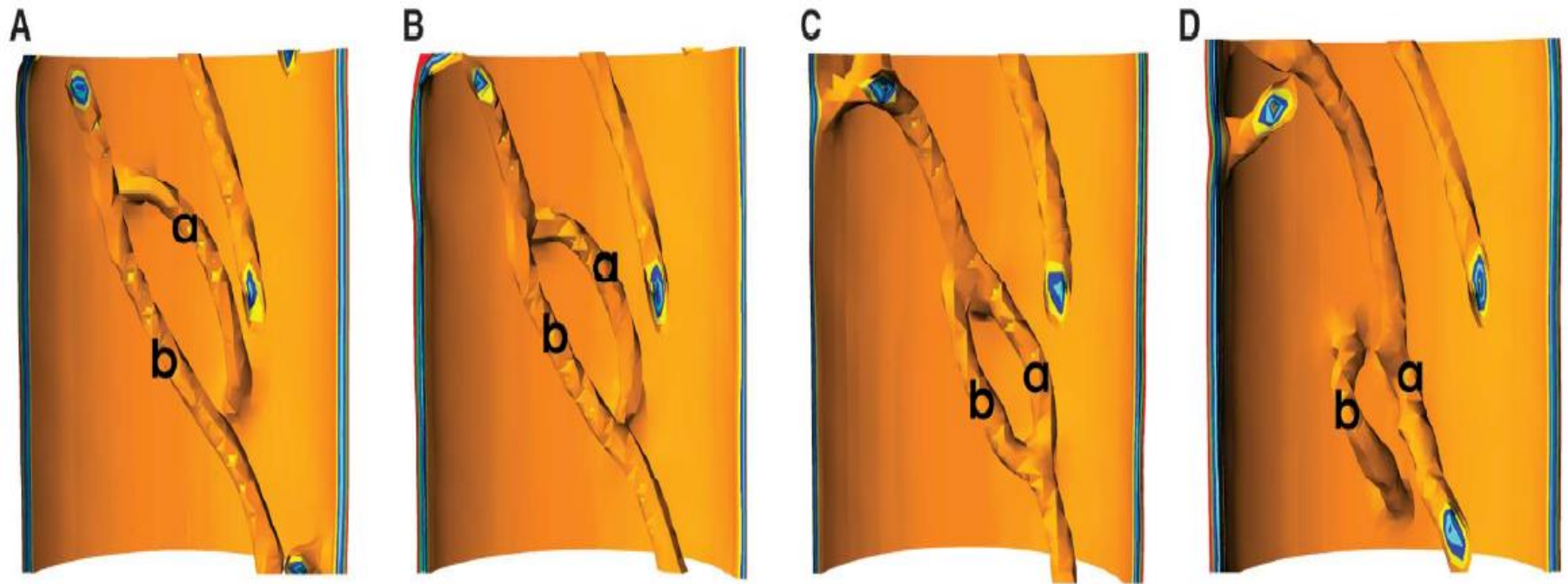


Fig. 3. (A to D) Two vortex lines approach each other, connect at two points, form a ring and exchange between them a portion of the vortex line, and subsequently separate. Segment (a), which initially belonged to the vortex line attached to the wall, is transferred to the long vortex line (b) after reconnection and vice versa.

Bulgac, Luo, Magierski, Roche, Yu, *Science* 332, 1288 (2011)

[More movies here: www.phys.washington.edu/groups/qmbnt/UFG/](http://www.phys.washington.edu/groups/qmbnt/UFG/)

A new method to construct the ground state which eschews big matrix diagonalization:

adiabatic switching with quantum friction

$$i\hbar\dot{\Psi}(x,t) = [H(x,t) + U(x,t)]\Psi(x,t)$$

$$E = \langle \Psi | H | \Psi \rangle$$

$$\dot{E} = \langle \Psi | \dot{H} | \Psi \rangle + \frac{2}{\hbar} \text{Im} \langle \Psi | HU | \Psi \rangle$$

$$\text{if } U \propto -\hbar \vec{\nabla} \cdot \vec{j} = \hbar \dot{\rho} \Rightarrow \dot{E} \leq \langle \Psi | \dot{H} | \Psi \rangle$$

$$\text{We choose } U = -\beta \frac{\hbar \vec{\nabla} \cdot \vec{j}}{\rho}$$

$$\vec{j}(\vec{r}) = \frac{\hbar}{m} \text{Im} \sum_n \psi_n^*(\vec{r}, t) \vec{\nabla} \psi_n(\vec{r}, t)$$

Main advantage:

Replace iterative procedure which requires $O(N^3)$ operations for diagonalization with time evolution which requires only $O(N^2 \ln(N))$ operations per time step.

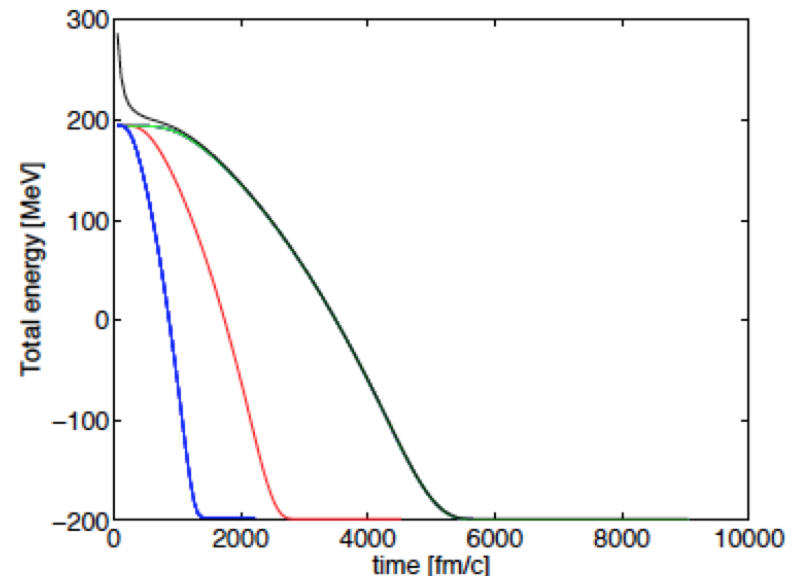


FIG. 2. (Color online) The total instantaneous energy of a system of twenty non-interacting neutrons evolving from an initial 3D harmonic oscillator potential to a final symmetrized Woods-Saxon potential. The curves correspond to quasi-adiabatic evolution with friction $(1 - s_t)H_0 + s_t H_1 + U_t$ for various switching periods T (two-thirds of the simulation time) and just friction $H_1 + U_t$ for the remaining third of the simulation. That the energy is constant during this time demonstrates that the ground state has been reached. Note: there are three curves for the longest T corresponding to different simulations with $\{24^3, 32^3, 40^3\}$ lattices of 1 fm spacing: this demonstrates the infrared (IR) convergence.

Papers we published so far on SLDA and TDSLDA

(stars indicate papers with significant nuclear physics content):

arXiv:1306.4266

* arXiv:1305.6891

* Phys. Rev. Lett. 110, 241102 (2013)

* Phys. Rev. C 87 051301(R) (2013)

* Ann. Rev. Nucl. Part. Phys. 63, 97 (2013)

* Phys. Rev. C 84, 051309(R) (2011)

Phys. Rev. Lett. 108, 150401 (2012)

Science, 332, 1288 (2011)

J. Phys. G: Nucl. Phys. 37, 064006 (2010)

Phys. Rev. Lett. 102, 085302 (2009)

Phys. Rev. Lett. 101, 215301 (2008)

* J.Phys. Conf. Ser. 125, 012064 (2008)

arXiv:1008.3933 chapter 9 in Lect. Notes Phys. vol. 836

Phys. Rev. A 76, 040502(R) (2007)

* Int. J. Mod. Phys. E 13, 147 (2004)

Phys. Rev. Lett. 91, 190404 (2003)

* Phys. Rev. Lett. 90, 222501 (2003)

* Phys. Rev. Lett. 90, 161101 (2003)

* Phys. Rev. C 65,051305(R) (2002)

* Phys. Rev. Lett. 88, 042504 (2002)

Plus a few other chapters in various books.